Gas-Phase Dissociation Pathways of Multiply Charged Peptide Clusters

John C. Jurchen, David E. Garcia, and Evan R. Williams
Department of Chemistry, University of California, Berkeley, California, USA

Numerous studies of cluster formation and dissociation have been conducted to determine properties of matter in the transition from the condensed phase to the gas phase using materials as diverse as atomic nuclei, noble gasses, metal clusters, and amino acids. Here, electrospray ionization is used to extend the study of cluster dissociation to peptides including leucine enkephalin with 7–19 monomer units and 2–5 protons, and somatostatin with 5 monomer units and 4 protons under conditions where its intramolecular disulfide bond is either oxidized or reduced. Evaporation of neutral monomers and charge separation by cluster fission are the competing dissociation pathways of both peptides. The dominant fission product for all leucine enkephalin clusters studied is a proton-bound dimer, presumably due to the high gas-phase stability of this species. The branching ratio of the fission and evaporation processes for leucine enkephalin clusters appears to be determined by the value of z^2/n for the cluster where z is the charge and n the number of monomer units in the cluster. Clusters with low and high values of z^2/n dissociate primarily by evaporation and cluster fission respectively, with a sharp transition between dissociation primarily by evaporation and primarily by fission measured at a z^2/n value of ~0.5. The dependence of the dissociation pathway of a cluster on z^2/n is similar to the dissociation of atomic nuclei and multiply charged metal clusters indicating that leucine enkephalin peptide clusters exist in a state that is more disordered, and possibly fluid, rather than highly structured in the dissociative transition state. The branching ratio, but not the dissociation pathway of $[\text{somatostatin}_5 + 4H]^{4+}$ is altered by the reduction of its internal disulfide bond indicating that monomer conformational flexibility plays a role in peptide cluster dissociation. (J Am Soc Mass Spectrom 2003, 14, 1373–1386) © 2003 American Society for Mass Spectrometry

Bulk properties of matter and the properties of isolated gas-phase atoms and molecules can have radically different characteristics in terms of structure, work function, ion solvation, etc. (for a review see reference [1]). One motivation behind cluster research is that the transitional characteristics between bulk and molecular properties can be discovered by studying intermediate states of matter. Investigators have explored a wide variety of materials, including charged droplets of various liquids [2, 3], clusters of noble metals [4–8], metal-ligand clusters [1, 9–11], highly charged clusters of noble gasses [12, 13], small molecules [14, 15], and ultra-cold clusters of transition metals [16]. Recently, investigators have formed noncovalently bound clusters of biologically important molecules, including clusters of amino acids and small peptides [17–28], and have studied their dissociation processes [18, 20, 26–28]. Multiply charged "clusters" of proteins consisting of multimeric, noncovalently associated protein complexes with a high degree of solution-phase structural specificity have been liberated into the gas phase [29–35]. From a simple mass measurement, the stoichiometry of the complex can be determined. There has also been much interest in determining if structural information can be inferred from gas-phase dissociation of the complexes [30, 33, 35, 36].

Gas-phase dissociation of a wide variety of clusters have been investigated [1–3, 5–8, 10–16, 18–20, 24, 26, 27, 30, 35–40]. In the case of multiply charged clusters, the two competing processes for dissociation are the evaporation of a neutral atom or molecule and the ejection of charged subunits. The latter occurs through a fission process in which the cluster dissociates into two or three charged fragments that then separate due to coulombic repulsion [41]. The competing processes of evaporation and fission have been described by various liquid-drop models for clusters as diverse as atomic nuclei [42], multiply charged metal clusters [5, 6], and highly charged solvent droplets [2, 3]. The recent development of femtosecond lasers capable of rapidly ionizing many molecules in atomic or molecular clusters has permitted access to another dissociation process whereby a cluster undergoes a coulombic explosion,

Published online October 20, 2003
Address reprint requests to Dr. E. R. Williams, Department of Chemistry, University of California, Berkeley, CA 94720-1460. E-mail: williams@cchem.berkeley.edu

1044-0305/03/$30.00
doi:10.1016/j.jasms.2003.07.003

Received May 30, 2003
Revised July 11, 2003
Accepted July 11, 2003

resulting in the isotropic ejection of many charged fragments [12–15].

General characteristics of cluster dissociation are well illustrated by multiply charged metal clusters. Evidence for their dissociation was first observed by Sattler et al. who, by measuring the mass and charge of Pb, Xe, and NaI clusters, observed half-integer cluster numbers that were interpreted to be doubly charged clusters [4]. It was found that the cluster size necessary to support two charges is much higher for Xe than for Pb or NaI due to the much weaker intermolecular attraction in Xe. Doubly charged Au clusters containing 9–17 atoms were isolated and collisionally activated by Saunders [5, 6]. These clusters were found to dissociate by competing mechanisms of neutral Au atom evaporation, and fission by the ejection of Au_3^+ and other products. Following collisional activation, larger Au clusters dissociate primarily by successive evaporation of neutral Au atoms while the smaller clusters, such as Au_{10}^{2+} and Au_9^{2+}, dissociate primarily through fission. Interestingly, the log of the ratio of the rates of fission to evaporation was found to vary linearly with z^2/n, where z is the cluster charge and n is the number of gold atoms in the cluster. This behavior corresponds closely to nuclear fission [43] and led Saunders to suggest that a similar liquid-drop model used to describe nuclear fission would also describe metal cluster dissociation [5, 6]. Recent work on the dissociation of noble metal clusters has shown that neutral evaporation and trimer fission are also the primary dissociation pathways of larger Au clusters and other metals [7, 8].

In contrast to the many cluster dissociation experiments that have been done with atoms and small molecules, only a few studies have been conducted with clusters of large, biologically relevant molecules. These have included studies of the dissociation and charge partitioning among the fragments of both homogeneous protein complexes that are biologically active in solution [29–35, 44, 45] and proteins that are nonspecifically aggregated [36, 44]. Studies have also been conducted on clusters of smaller, biologically relevant molecules, and these have tended to focus on amino acids and small peptides. Amino acid and peptide clusters can be readily formed by electrospray ionization (ESI) and initial reports were concerned with clusters of monomers (M) of the form $[M_n + nH]^{n+}$ that appear at the same nominal *m/z* as the singly protonated monomer. These ions are indistinguishable in low resolution mass spectra from the monomer and larger clusters and could potentially complicate the interpretation of dissociation spectra [17, 19, 21, 23, 46]. While the formation of such highly charged molecular clusters by ESI is interesting in its own right and indicative of the gentle nature of the ESI process, the elucidation of dissociation pathways for clusters of the type $[M_n + nH]^{n+}$ is more complicated as the fragments are likely to be at the same *m/z* as the parent ion.

Some observations have been made of amino acid and peptide clusters formed by ESI of the type $[M_m + nH]^{n+}$ where $m > n$ [18, 20, 22–28, 40, 47]. Much of this work has focused on octamers of the amino acid serine that have been found to form with a preference for homochirality [20, 22, 25–27, 48]). Clusters of serine as large as $[44Ser + 4H]^{4+}$ were isolated by Beauchamp and coworkers and collisionally activated in an ion trap mass spectrometer [20]. The cluster dissociation revealed that the large serine clusters dissociate by a combination of fission and evaporation, but the specific dissociation pathways are difficult to determine because the primary fragment ions of noncovalently bound complexes are often sufficiently activated to undergo subsequent dissociation. For example, although the activation of $[30Ser + 3H]^{3+}$ was shown to produce a dissociation spectrum with fragments ranging in size from $[23Ser + 3H]^{3+}$ to $[29Ser + 3H]^{3+}$ [20], it is not known whether the fragments are a result of sequential evaporation of single amino acids or if several dissociation pathways exist whereby different sizes of neutral serine clusters evaporate from the original cluster. Because the primary activation products are more likely to provide the most information about the structure of the initial cluster, it is important to distinguish between primary and secondary fragments. A useful technique for distinguishing between primary and secondary dissociation products is double resonance (DR).

DR was initially developed to identify chemically coupled processes in equilibrium experiments conducted in ion cyclotron resonance mass spectrometers [49] and was later adapted for Fourier-transform mass spectrometry [50] and other kinds of mass spectrometry [51]. DR experiments are done by applying an on-resonance ejection waveform simultaneous with the dissociation event, with the aim of ejecting primary fragment ions before they undergo subsequent dissociation. If the ejection of an ion perturbs the abundance of another ion, it indicates that the second ion is formed by subsequent dissociation of the ejected ion and not directly from the activated precursor ion.

In this work, the dissociation pathways of multiply charged peptide clusters of leucine enkephalin and both oxidized and reduced somatostatin are elucidated using collisionally activated dissociation and DR. The effects of cluster size and charge on the dissociation pathways of leucine enkephalin clusters are compared with the dissociation of multiply charged metal clusters. To the authors' knowledge, this is the first application of DR to multiply charged cluster dissociation.

Experimental

Mass Spectrometry

The experiments were conducted on a 110 mm bore 9.4 T Fourier-transform mass spectrometer that was constructed in collaboration with Bruker Daltonics (Billerica, MA) (Figure 1). This instrument has been described elsewhere [36]. The ion optics and introduction

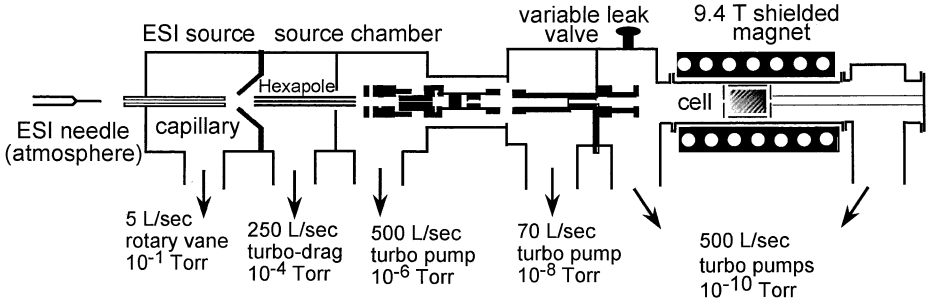

Figure 1. Diagram of the 9.4 tesla Berkeley-Bruker Fourier-transform mass spectrometer.

system are a standard Bruker design. Ions are generated by nanoelectrospray using borosilicate capillaries that are pulled to a ~4 μm tip with a model P-87 capillary puller (Sutter Instruments, Novato, CA). A small volume of sample solution (4-10 μL) is loaded into the borosilicate capillary and a platinum wire is inserted into the solution at the end of the capillary. The capillary is positioned ~2 mm from the source inlet and a potential of ~900 V is applied to the platinum wire.

The electrospray generated ions are accumulated in a storage hexapole prior to injection through multiple ion lenses and three stages of differential pumping into the ultra high vacuum chamber (3×10^{-9} torr) of the instrument where the ions are trapped in a cylindrical Bruker Infinity cell. Each ion injection is accompanied by a pulse of nitrogen gas introduced into the vacuum chamber at a pressure of $\sim 2 \times 10^{-6}$ torr to enhance trapping and to damp the motion of the ions in the cell.

Chemicals

Leucine enkephalin (Tyr-Gly-Gly-Phe-Leu), somatostatin (Ala-Gly-Cys-Lys-Asn-Phe-Phe-Trp-Lys-Thr-Phe-Thr-Ser-Cys [Disulfide bridge: 3–14]) and dithiolthreitol (DTT) were purchased from Sigma-Aldrich C. (St. Louis, MO) and were used without further treatment except for the disulfide reduction described below. Methanol and acetic acid (99.9%) were purchased from EM Science (Gibbstown, NJ) and from Fisher Scientific (Pittsburgh, PA) respectively.

Disulfide Bond Reduction

For each day of experiments, a fresh solution with a concentration of 5 mM somatostatin (ST) and 50 mM DTT was made in Millipore 18.2 MΩ H_2O. The solution was placed in a sealed eppendorf tube covered with parafilm, and heated in a water bath at 80–95 °C for ~50 min. Disulfide reduction was nearly complete as verified by an average increase of 2 Da in the peptide mass following the reduction procedure. ST remained reduced for several hours following the reduction procedure. Fresh, reduced solutions of ST were prepared for each day of experiments.

Cluster Formation

Solutions of leucine enkephalin (LE) and oxidized ST for ESI were prepared at concentrations of ~2.5 and ~1.3 mM, respectively, in 1:1 water:methanol + 2 % acetic acid by volume. The relatively high peptide concentrations were found to enhance cluster formation. Solutions of reduced ST for ESI were prepared by diluting stock solutions of 5 mM somatostatin and 50 mM DTT to final concentrations of 1.3 mM and 13 mM, respectively, in 1:1 water:methanol + 2 % acetic acid. In order to stabilize the nanoelectrospray emission, ammonium acetate was added to the reduced ST solution containing 13 mM DTT until the final concentration was 100 mM. This technique is often useful for obtaining nanoelectrospray signal from solutions containing a high concentration of small molecules, such as DTT, which often result in unsteady nanoelectrospray currents.

The signal intensity of peptide clusters is enhanced by tuning for selective accumulation in the external hexapole of the instrument. This is done by accumulating the ions in the hexapole for 3 s (versus $\leq$ 1.0 s typically), increasing the hexapole dc offset from ~2.7 to 3.5–4.5 V and injecting multiple hexapole accumulations into the ion cell prior to detection. The particular clusters measured in the mass spectra using a given set of tuning conditions are also sensitive to the voltage applied to the nanoelectrospray needle. In general, slowly decreasing the applied nanoelectrospray voltage after initiating ion current favors the formation of larger clusters. By tuning the hexapole offset and the second skimmer potentials and adjusting the electrospray voltage, it is possible to dramatically change the appearance of the mass spectra so that the abundance of a cluster of interest is greatly enhanced.

Double Resonance and Collisional Activation

Modifications to the electronics of the APEX II mass spectrometer were implemented in order to do DR experiments. An additional transmitter board and a HI-222 analog switch from Bruker Daltonics were installed in the high frequency unit of the APEX II mass spectrometer. Modifications to the multiplexer board of

the mass spectrometer were made in-house according to specifications provided by Scott Daniels (Bruker Daltonics, Billerica MA) that permit two excite frequencies to be applied simultaneously to ions in the cell of the mass spectrometer. The software to implement DR experiments is a modification of code written by Dr. Christian Berg (Bruker Daltonics, Billerica MA).

Peptide clusters of interest were isolated using two identical correlated sweeps with a pulse of nitrogen gas introduced into the ion cell between the sweeps. Following the double isolation, the clusters were dissociated by sustained off-resonance irradiation collisionally activated dissociation (SORI-CAD) [52] in which an excitation waveform was applied +600 Hz off-resonance for two seconds with an applied peak-to-peak potential of 6–10 V. A pulse of nitrogen gas was introduced for 90 ms, briefly raising the pressure to ~2 $\times 10^{-6}$ torr. During DR experiments, a second excitation waveform is applied on-resonance to the fragment ion under investigation for the duration of the SORI excitation and for an additional 1.0 s to eject fragment ions that continue to dissociate after the SORI waveform is turned off. The amplitude of the DR waveform was adjusted to eject the fragment ions as rapidly as possible while avoiding additional excitation of the precursor ion or any of the other fragment ions. The maximum voltage that could be applied without additionally exciting the precursor or other fragment ions varied from 4–32 V pk–pk depending on the *m/z* and the proximity of other fragment ions of the DR waveform.

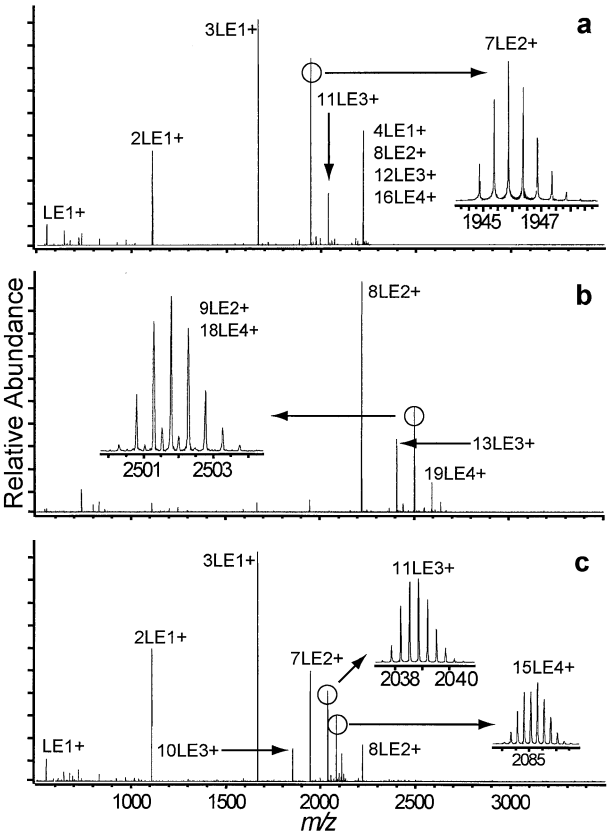

Figure 2. Nanoelectrospray mass spectra of 2.5 mM LE in 1:1 water:methanol + 2% acetic acid with electrospray voltage and hexapole accumulation parameters optimized for maximal ion intensity of the (**a**) $7LE^{2+}$, (**b**) $9LE^{2+}$, and (**c**) $11LE^{3+}$ and $15LE^{4+}$ clusters.

Results

Multiply charged, gas-phase noncovalent clusters of leucine enkephalin (LE) and somatostatin (ST) can be readily formed from concentrated solutions using nanoelectrospray ionization. The gas-phase dissociation pathways of these clusters were investigated using collisional activation and double resonance (DR) ejection. Many of the primary fragment ions produced from the dissociation of these clusters have sufficient internal energies to undergo further fragmentation before ion detection making DR experiments useful for determining dissociation pathways. In DR experiments, one of the fragment ions resulting from dissociation of a precursor cluster ion is continuously ejected from the ion cell while the precursor ion is activated. If subsequent dissociation of the fragment ion requires more time than ion ejection (~3–24 ms for these experiments depending on the amplitude of the DR ejection pulse), the products of this ion will not appear in the DR spectrum. Thus, secondary dissociation products are identified by their decrease in abundance when a DR waveform is applied to eject their parent ion. Dissociation pathways for several different clusters of LE and one cluster of ST with its individual peptides containing either oxidized or reduced disulfide bonds are described in the following sections.

It should be noted that each cluster ion is isolated by two correlated sweeps with a pulse of gas between the sweeps. After an initial correlated sweep, the isolated cluster undergoes some dissociation after a pulse of nitrogen collision gas is introduced. When the cluster is re-isolated by a second, identical correlated sweep, the remaining ions do not dissociate as readily. This result suggests that either the nonspecific peptide clusters examined in this study exist in more than one gas-phase configuration that have different stabilities or that the ions are kinetically excited after trapping. The clusters investigated in this study are those that survive the double isolation.

Leucine Enkephalin 7-Mer^{2+}

Doubly protonated LE clusters consisting of seven monomers ($7LE^{2+}$) are readily formed by nanoelectrospray (Figure 2a). Dissociation of $7LE^{2+}$ (Figure 3a) results in abundant LE^+ and $2LE^+$ ions along with lower abundance $3LE^+$, $4LE^+$, and $5LE^+$ ions. Interestingly, the abundance of $2LE^+$ greatly exceeds that of its complimentary ion, $5LE^+$, and the complimentary ion to LE^+, $6LE^+$, is absent from the dissociation spectrum. Although mass discrimination may account for a very

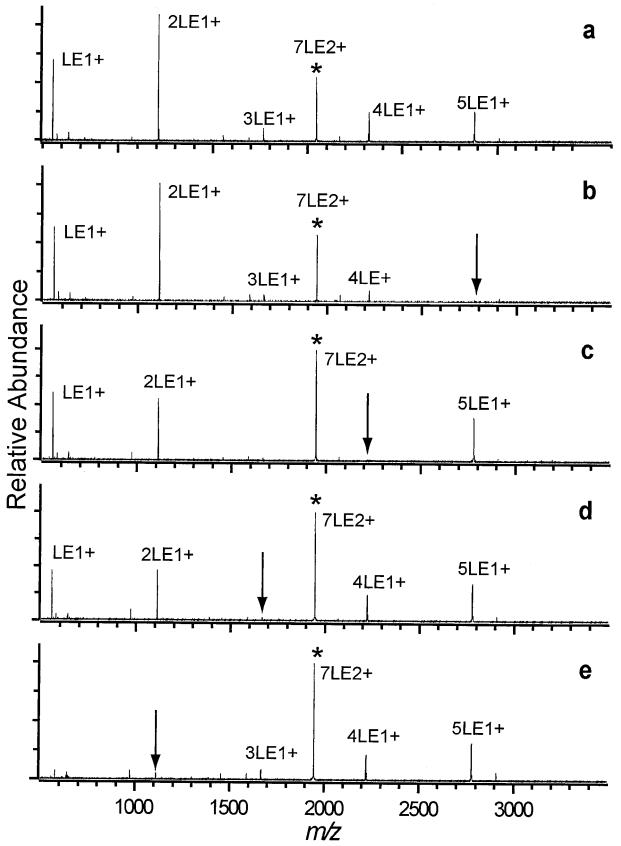

Figure 3. Sustained off-resonance irradiation collisionally activated dissociation (SORI-CAD) spectra of the $7LE^{2+}$ cluster (**a**) without double resonance (DR) and with DR ejection applied at the *m/z* corresponding to the (**b**) $5LE^{+}$, (**c**) $4LE^{+}$, (**d**) $3LE^{+}$, and (**e**) $2LE^{+}$ clusters.

small fraction of the asymmetry observed, secondary fragmentation accounts for the majority. Application of a DR ejection pulse to the *m/z* corresponding to $6LE^{+}$ causes no change in the appearance of the mass spectrum indicating that $6LE^{+}$ is not a significant dissociation product of $7LE^{2+}$. When a DR ejection pulse is applied to the $5LE^{+}$ peak (Figure 3b), the abundance of the other fragmentation peaks change considerably. The abundance of $4LE^{+}$ and $3LE^{+}$ are attenuated, suggesting that a substantial fraction of these ions are formed by subsequent dissociation of the primary $5LE^{+}$ fragment. Application of a DR waveform at the frequency of the $4LE^{+}$ ion (Figure 3c) results in a further attenuation of $3LE^{+}$ and $2LE^{+}$ ions. The isotopic distribution of the $3LE^{+}$ peak shows that $6LE^{2+}$ is present in the dissociation spectra with an intensity as high as 10% of the $3LE^{+}$ peak indicating that the $7LE^{2+} \rightarrow 6LE^{2+} + LE^{0}$ process does occur. The abundance of $6LE^{2+}$ varies considerably from scan to scan and is often not detectable within the signal to noise of the experiment. Based on the observed abundance of the $6LE^{2+}$ peak, the $7LE^{2+} \rightarrow 6LE^{2+} + LE^{0}$ process does not constitute more than ~0.005% of the total dissociation.

The $4LE^{+}$ and $3LE^{+}$ peaks can be formed by two possible dissociation processes. Either the $3LE^{+}$ peak is formed by evaporation of neutral LE from larger, singly charged clusters, or it is formed by symmetric fission of $7LE^{2+}$ to form complimentary $3LE^{+}$ and $4LE^{+}$. The results of the DR experiments indicate that most, if not all, of the $4LE^{+}$ and $3LE^{+}$ are formed by subsequent LE evaporation from $5LE^{+}$. Ejection of $5LE^{+}$ (Figure 3b) greatly attenuates the $4LE^{+}$ and $3LE^{+}$ abundance, indicating that the $5LE^{+} \rightarrow 4LE^{+} \rightarrow 3LE^{+}$ pathway does occur. DR ejection of the $4LE^{+}$ (Figure 3c) virtually eliminates the $3LE^{+}$, and the $2LE^{+}$ and LE^{+} peaks are attenuated. DR ejection of the $3LE^{+}$ (Figure 3d) leads to the same attenuation of $2LE^{+}$ and LE^{+}, as DR ejection of $4LE^{+}$ (Figure 3c), strongly suggesting that $7LE^{2+} \rightarrow 4LE^{+} + 3LE^{+}$ does not occur. If $7LE^{2+} \rightarrow 4LE^{+} + 3LE^{+}$ did occur, DR ejection of the $3LE^{+}$ would be expected to cause additional attenuation of $2LE^{+}$ and LE^{+}. Thus, the majority of $4LE^{+}$ and $3LE^{+}$ in Figure 3b occurs due to $5LE^{+}$ undergoing rapid dissociation during the ~3 ms required to eject the protonated $5LE^{+}$ from the ion cell. Ejection of $2LE^{+}$ virtually eliminates the peak corresponding to LE^{+} indicating that LE^{+} is not a significant primary fragment ion. A summary of the dissociation pathways of $7LE^{2+}$ deduced from these DR experiments is depicted in Scheme **1**.

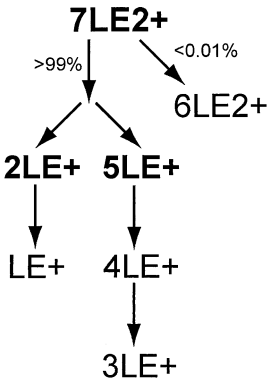

Scheme 1

Leucine Enkephalin 9-Mer^{2+}

A slight adjustment of the hexapole accumulation parameters and the voltage applied to the nanoelectrospray needle causes a dramatic shift in the relative peak intensities of the LE cluster ions, such that the abundance of $9LE^{2+}$ greatly exceeds that of $7LE^{2+}$ (Figure 2b). The isotopic distribution of $9LE^{2+}$ indicates the presence of $18LE^{4+}$ (Figure 2b inset). Both $9LE^{2+}$ and $18LE^{4+}$ are activated during SORI excitation and some products from dissociation of $18LE^{4+}$ are apparent as indicated by the appearance of $16LE^{3+}$ formed by the pathway $18LE^{4+} \rightarrow 16LE^{3+} + 2LE^{+}$. Unlike $9LE^{2+}$, which dissociates into many fragments by multiple pathways, $18LE^{4+}$ appears to dissociate only by the ejection of $2LE^{+}$. The $16LE^{3+}$ does not appear to undergo further dissociation as DR ejection changes the appearance of other peaks in the spectrum very little

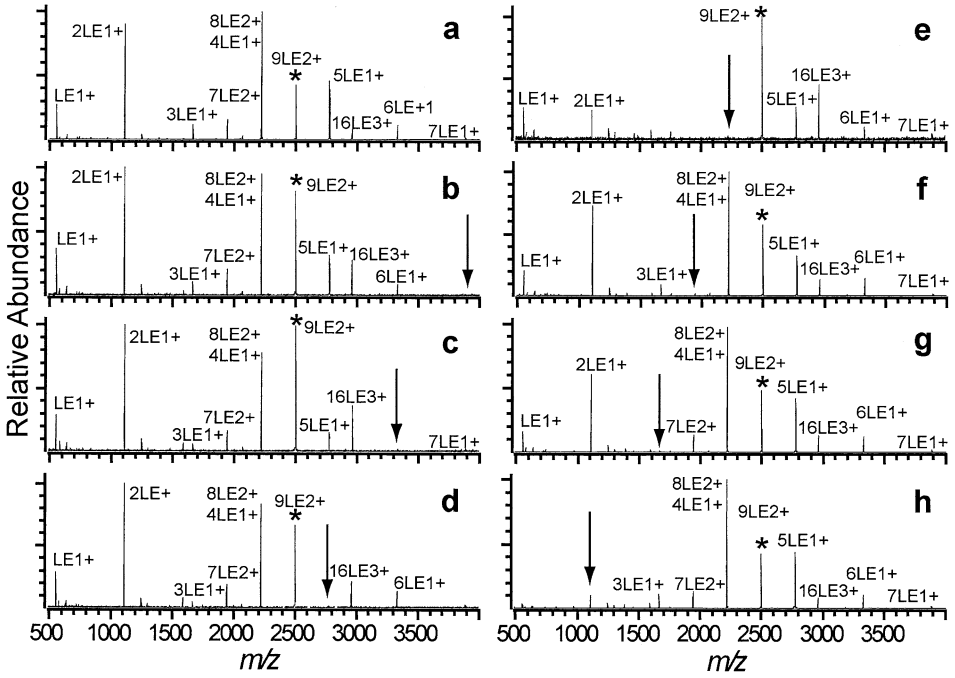

Figure 4. SORI-CAD spectra of the $9LE^{2+}$ cluster (**a**) without DR and with DR ejection applied at the *m/z* corresponding to the (**b**) $7LE^{+}$, (**c**) $6LE^{+}$, (**d**) $5LE^{+}$, (**e**) $8LE^{2+}/4LE^{+}$, (**f**) $7LE^{2+}$, (**g**) $3LE^{+}$, and (**h**) $2LE^{+}$ clusters.

(data not shown). It should be noted that the ratio of $9LE^{2+}$ and $18LE^{4+}$ varied during the DR experiment, resulting in a slight variation in the relative abundance of $16LE^{3+}$ to the other fragment clusters.

Unlike the $7LE^{2+}$, which dissociates almost entirely by fission, $9LE^{2+}$ dissociates by a combination of evaporation and fission processes. The dissociation spectrum of $9LE^{2+}$ (Figure 4a) shows that a large number of cluster fragments are formed. The most abundant of these is the $8LE^{2+}/4LE^{+}$ peak. Although $8LE^{2+}$ and $4LE^{+}$ have the same nominal *m/z*, the isotopic distribution indicates that while both clusters are present, approximately 70% of the peak is $8LE^{2+}$, produced directly from $9LE^{2+}$ by the evaporation of neutral LE. A comparison of Figure 4a and e shows that double resonance ejection of $8LE^{2+}$ results in the elimination of $7LE^{2+}$ and $3LE^{+}$ and a decrease in the relative abundance, compared to the parent ion, of all other fragment clusters except for $16LE^{3+}$ and $7LE^{+}$. The abundance of $7LE^{2+}$ and $3LE^{+}$ during DR ejection of $8LE^{2+}$ indicates that $7LE^{2+}$ is formed by two consecutive losses of neutral LE from $9LE^{2+}$ and that $3LE^{+}$ is formed by neutral loss from $4LE^{+}$. The decrease in abundance of $5LE^{+}$ and $6LE^{+}$ during DR ejection of $8LE^{2+}$ indicates that after dissociation by the $8LE^{2+} \rightarrow 2LE^{+} + 6LE^{+}$ pathway, $6LE^{+}$ can undergo neutral loss to form $5LE^{+}$. Note that the abundance of $6LE^{+}$ normalized to $9LE^{2+}$ is significantly attenuated by a DR pulse on $8LE^{2+}$ (Figure 4e) from the abundance of $6LE^{+}$ normalized to $9LE^{2+}$ in the regular activation spectrum (Figure 4a). It is evident that very little LE^{+} is formed directly from the $8LE^{2+}$ as the ejection of $2LE^{+}$ virtually eliminates LE^{+} (Figure 4h). DR ejection of $7LE^{+}$, $6LE^{+}$ and $5LE^{+}$ all cause decrease in signal and a change in the isotopic distribution for $8LE^{2+}/4LE^{+}$ indicating that the $4LE^{+}$ in the $8LE^{2+}/4LE^{+}$ peak is primarily produced by evaporation of neutral LE from larger singly charged clusters. DR ejection of $7LE^{2+}$ (Figure 4f) alters the relative abundance of the peaks in the spectra very little except for a small decrease in $5LE^{+}$ and $2LE^{+}$ suggesting that the $9LE^{2+} \rightarrow 8LE^{2+} \rightarrow 7LE^{2+} \rightarrow$ (fragments) pathway is not a dominant process under the dissociation conditions used.

The relative branching ratios for the evaporation and fission dissociation processes were approximated by comparing the spectra for activation of $9LE^{2+}$ and DR ejection of $8LE^{2+}$ (Figure 4a, e). Specifically, the intensities of the fragment ions in Figure 4e were normalized to the parent ion and summed to represent the total fission process as any ions formed by LE evaporation from $9LE^{2+}$ would have been ejected by the DR waveform. The approximate percentage of fission was then determined by dividing the normalized intensity of all peaks resulting exclusively from fission of the parent ion (Figure 4e) by the total normalized intensity of all the fragment peaks in the initial activation spectrum (Figure 4a). The resulting quotient indicates ~13% dissociation by fission. This method slightly underestimates fission dissociation as a portion of the $4LE^{+}$ ion ejected during the DR pulse is formed by sequential evaporation of neutral LE from the primary fragment ion $7LE^{+}$. The $7LE^{+}$ ion is formed by the $9LE^{2+} \rightarrow 2LE^{+} + 7LE^{+}$ process as indicated by the decrease in the $8LE^{2+}/4LE^{+}$ peak when a DR waveform is applied to

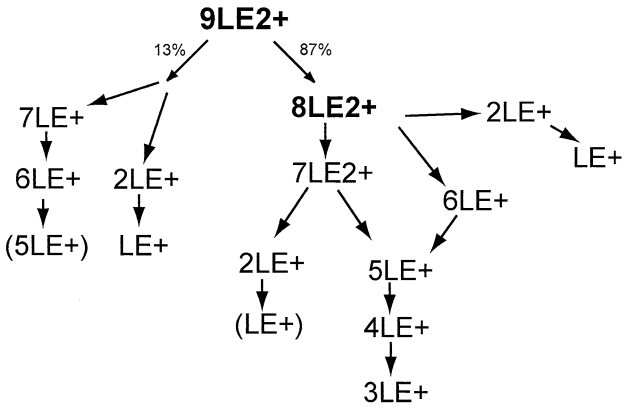

Scheme 2

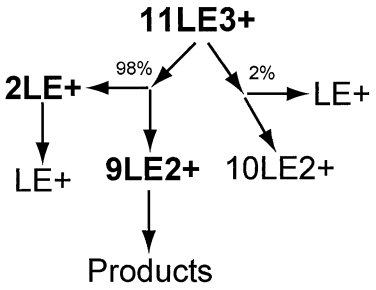

Scheme 3

7LE$^+$ (Figure 4b). A summary of the dissociation pathways of 9LE^{2+} deduced from these DR experiments is presented in Scheme **2**.

Leucine Enkephalin 11-Mer^{3+}

The hexapole accumulation and nanoelectrospray voltage can be tuned to produce a high abundance of 11LE^{3+} and 15LE^{4+} (Figure 2c). The activation spectrum of 11LE^{3+} is much simpler than that for 9LE^{2+} (Figure 5a). As in the case of 7LE^{2+}, the primary dissociation pathway is asymmetric fission, specifically the ejection of a proton-bound dimer, 2LE$^+$, and complimentary 9LE^{2+}. The subsequent dissociation of 9LE^{2+} by the evaporation of a neutral to form the 8LE^{2+} and by fission and subsequent evaporation to form 5LE$^+$ and 4LE$^+$ is consistent with the dissociation pathways of the 9LE^{2+} cluster discussed above. The peak labeled 10LE^{2+}/5LE$^+$ is identified as a combination of the two clusters by the isotopic distribution. The formation of 10LE^{2+} from 11LE^{3+} indicates that the 11LE^{3+} cluster also dissociates by a highly asymmetric fission process ejecting LE$^+$. This is clearly a minor pathway with a branching ratio of no more than 2%, and is difficult to measure in spectra with poor signal to noise (as in Figure 5c, d). It should be noted that ideally, the relative peak intensity for Fourier-transform mass spectrometry is proportional to the charge of the ions under investigation. For example, an equal number of 9LE^{2+} and 2LE$^+$ ions would produce a relative peak intensity ratio of 2:1 for 9LE^{2+} and 2LE$^+$. Even considering the effect of charge, the sum of the intensities for the 2LE$^+$ and LE$^+$ is more than half of the sum of the intensities of the 9LE^{2+}, 5LE$^+$/10LE^{2+}, and 8LE^{2+} peaks (Figure 5a). This indicates that there is a slight mass bias towards lower *m/z* ions.

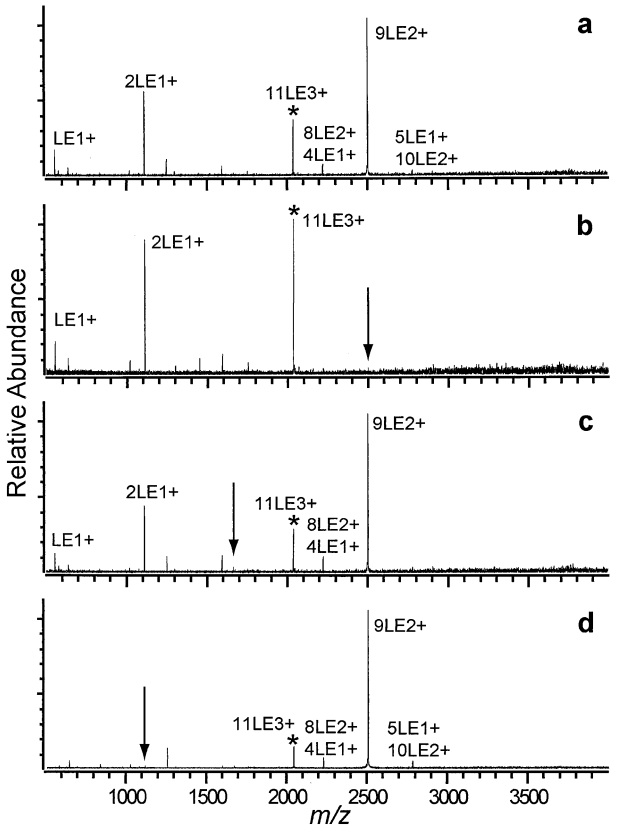

Figure 5. SORI-CAD spectra of the 11LE^{3+} cluster (**a**) without DR and with DR ejection applied at the *m/z* corresponding to the (**b**) 9LE^{2+}, (**c**) 3LE$^+$, and (**d**) 2LE$^+$ clusters.

DR ejection of 9LE^{2+} eliminates 8LE^{2+} indicating that the same 9LE^{2+} $\rightarrow$ 8LE^{2+} + LE^0 dissociation pathway measured for the 9LE^{2+} cluster occurs. Ejection of 9LE^{2+} may also decrease the relative abundance of 2LE$^+$ slightly, suggesting that 2LE$^+$ is formed from either 9LE^{2+} or 8LE^{2+}, which is consistent with the DR experiments mentioned above (Figure 5b). As observed in the case of both 7LE^{2+} and 9LE^{2+}, protonated LE is formed primarily from 2LE$^+$ (Figure 5d). A summary of the dissociation pathways of 11LE^{3+} deduced from these DR experiments is presented in Scheme **3**.

Leucine Enkephalin 15-Mer^{4+}

The 15LE^{4+} cluster is highly fissionable and difficult to isolate, as evidenced by a small amount of 13LE^{3+} formed by collisional excitation during the isolation procedure (Figure 6a). Activation of 15LE^{4+} results in a number of dissociation products from both fission and evaporation processes (Figure 6b). The primary dissociation process of 15LE^{4+} is the ejection of 2LE$^+$ to form

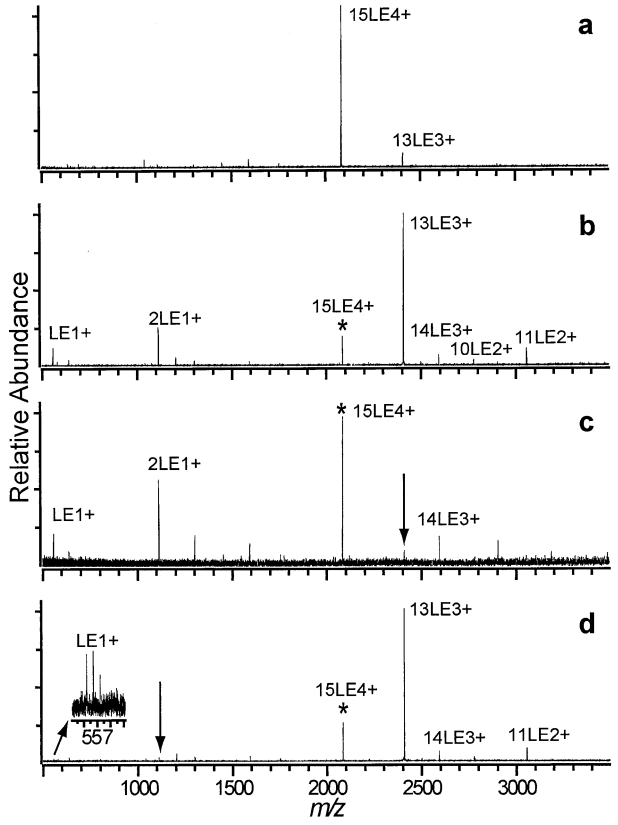

Figure 6. SORI-CAD spectra of the $15LE^{4+}$ cluster (**a**) isolation spectrum and activation spectra (**b**) without DR and with DR ejection applied at the *m/z* corresponding to the (**c**) $13LE^{3+}$ and (**d**) $2LE^{+}$ clusters.

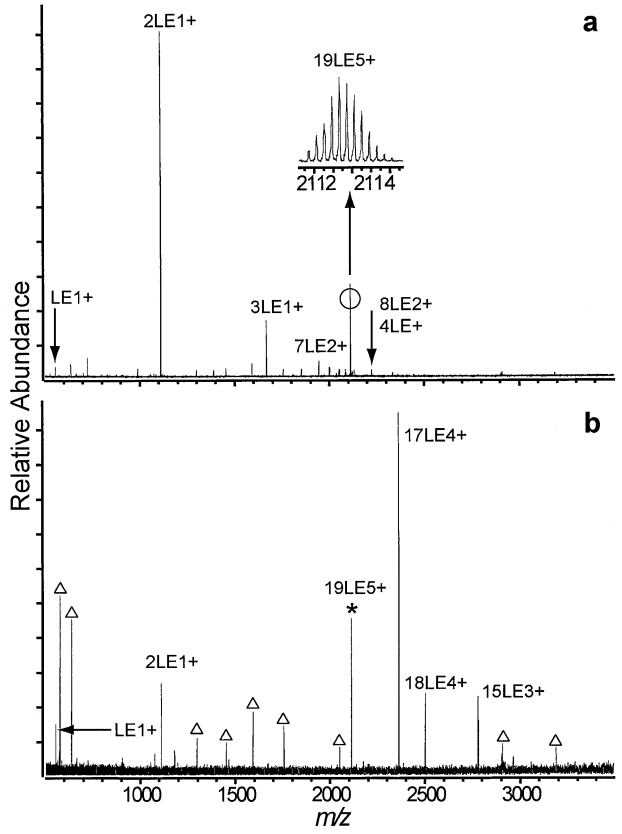

Figure 7. Nanoelectrospray mass spectra of 2.5 mM LE in 1:1 water:methanol + 2% acetic acid with electrospray voltage and hexapole accumulation parameters optimized for maximal ion intensity of the (**a**) $19LE^{5+}$ cluster and (**b**) a SORI-CAD spectrum of the isolated $19LE^{5+}$ cluster.

$13LE^{3+}$ which undergoes further dissociation by the ejection of $2LE^{+}$ to form $11LE^{2+}$ (Figure 6c). Formation of $10LE^{2+}$ occurs by the evaporation of a neutral LE from $11LE^{2+}$. This was confirmed by another isolation experiment showing that $11LE^{2+}$ dissociates by the evaporation of neutral LE to form $10LE^{2+}$ and also by a minor fission process ejecting $2LE^{+}$ (data not shown). The $15LE^{4+}$ precursor dissociates by another competing fission process as well, ejecting LE^{+} to form $14LE^{3+}$. This asymmetric dissociation process is also measured for $11LE^{3+}$ but has a higher branching ratio for $15LE^{4+}$ contributing ~6% to the total dissociation (Scheme **4**).

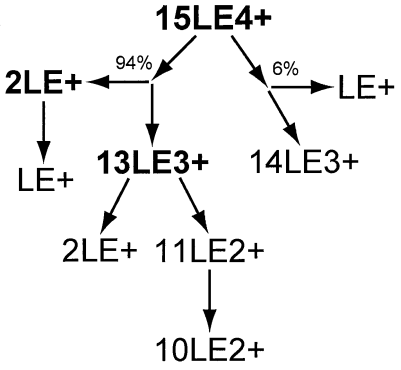

Scheme 4

Leucine Enkephalin 19-Mer^{5+}

After further hexapole accumulation and nanoelectrospray voltage adjustment, it is possible to form large clusters, such as $19LE^{5+}$, with high abundance (Figure 7a). There is considerable variation in the abundance of $19LE^{5+}$ in the mass spectra with different pulled nanoelectrospray capillaries, and the relative abundance of $19LE^{5+}$ varied with time. Additional noise in the spectra is due to the installation of a resistance temperature device to measure the temperature of the vacuum chamber in the vicinity of the ion cell for another series of experiments (Figure 7b).

Although DR ejection was not done for $19LE^{5+}$, the dissociation pathways are easily interpreted and are consistent with those of the smaller LE clusters. The primary dissociation pathway for $19LE^{5+}$ is the ejection of $2LE^{+}$ to form $17LE^{4+}$. The $17LE^{4+}$ cluster undergoes fission by the ejection of another $2LE^{+}$ to form $15LE^{3+}$. Similar to the $15LE^{4+}$ and $11LE^{3+}$ cluster dissociation, ejection of LE^{+} from $19LE^{5+}$ competes with ejection of $2LE^{+}$. This highly asymmetric process is increasingly

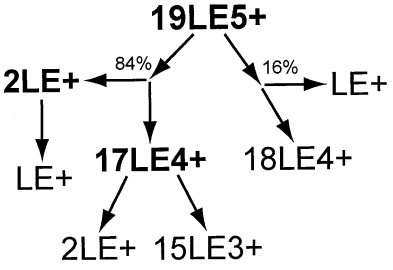

Scheme 5

dominant with $19LE^{5+}$, and constitutes approximately 16% of the total dissociation. The proposed dissociation pathways are presented in Scheme **5**.

Somatostatin 5-Mer^{4+} Clusters

To determine the effect of monomer flexibility on the peptide dissociation process, peptide clusters were formed with the intramolecular disulfide bond of ST either oxidized or reduced. This also provided an opportunity to examine the dissociation pathways of a peptide with a higher charge-to-subunit ratio. A smaller range of cluster sizes are formed for ST than for LE, and these experiments focus exclusively on the $[somatostatin_5 + 4H]^{4+}$ ($5ST^{4+}$) cluster (Figure 8a, b). The native form of the peptide has a disulfide bond between residues 3 and 14. Intramolecular disulfide bonds are important in determining both the gas-phase structure of somatostatin [53] and gas-phase conformational flexibility [36]. The addition of DTT into ST solutions resulted in a reduction of an average of 4 out of 5 disulfide bonds present in each cluster as indicated by the shift in mass of two Da for each disulfide bond reduced (data not shown).

Upon SORI activation, oxidized $5ST^{4+}$ clusters dissociate by competing processes of neutral monomer evaporation and fission by the ejection of a protonated monomer (Figure 8b). Following disulfide bond reduction, identical dissociation pathways are measured (Figure 8a), but a different branching ratio is observed. The $4ST^{3+}$ fission product undergoes secondary dissociation by competing fission and evaporation processes. Subsequent sequential fission by the ejection of protonated monomers form $3ST^{2+}$ (Figure 8c) and $2ST^{+}$ (Figure 8d). The intensity of the ST^{+} peak is much higher than would be expected if its formation was due exclusively to fission of $5ST^{4+}$ as the charge-normalized ST^{+} peak would be expected to be roughly 1/3 the intensity of $4ST^{3+}$. The high abundance of ST^{+} indicates that a fraction of these ions must be formed by other dissociation pathways. The DR experiments show that the following processes occur: $5ST^{4+} \rightarrow 4ST^{4+} + ST^{0}$, $4ST^{3+} \rightarrow 3ST^{3+} + ST^{0}$, and $3ST^{2+} \rightarrow 2ST^{2+} + ST^{0}$. The product cluster ions formed by these reactions, $4ST^{4+}$, $3ST^{3+}$, and $2ST^{2+}$, must completely dissociate into singly charged monomers. An analysis of the isotopic distribution of ST^{+} formed by the dissociation of $5ST4^{+}$ shows that higher order aggregates of ST^{+} are not detectable, so they constitute no more than 0.5% of the peak intensity of ST^{+}. DR experiments demonstrate that the dissociation pathways of reduced $5ST^{4+}$ are the same as those of the corresponding oxidized cluster (data not shown).

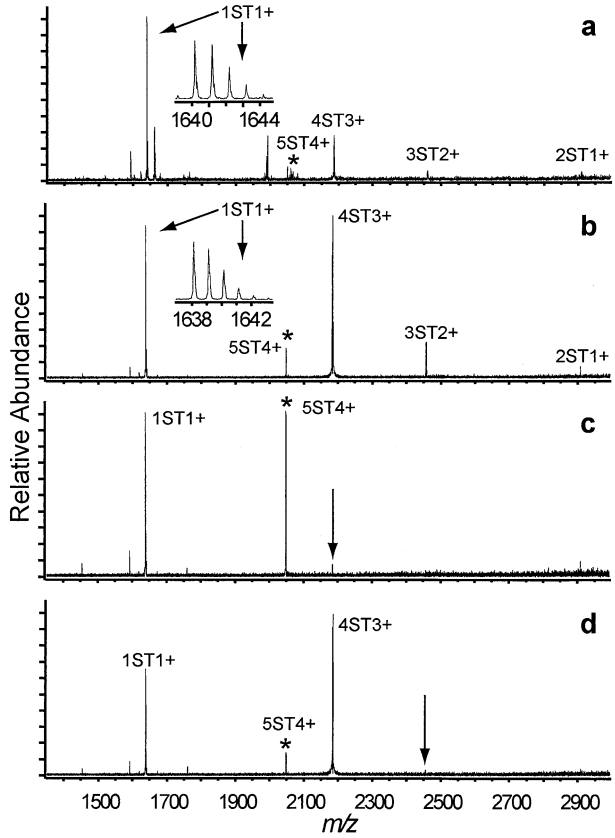

Figure 8. SORI-CAD spectra of the $5ST^{4+}$ with its intramolecular disulfide bonds (**a**) reduced and (**b**) oxidized and with DR ejection applied during activation of oxidized $5ST^{4+}$ at the *m/z* corresponding to (**c**) $4ST^{3+}$ and (**d**) $3ST^{2+}$. Inset spectra in (**a**) and (**b**) are transformed from apodized data to show the absence of higher order/charged clusters at these *m/z* values.

Discussion

Structure of Peptide Clusters

An important question in cluster experiments with biological molecules is whether structure can be deduced from dissociation experiments. While it does not seem possible to extract a detailed analysis of the structure of leucine enkephalin (LE) and somatostatin (ST) clusters from the MS/MS and DR results mentioned above, it seems reasonable to suggest some general characteristics of the clusters in question based on the dissociation products and pathways of LE and ST.

It seems that the stability of the proton-bound dimer ($2LE^{+}$) is the driving force behind the dissociation processes for the LE clusters studied. Ejection of $2LE^{+}$ is

by far the most dominant fission product for all multiply charged LE clusters investigated, and for larger clusters, such as the $15LE^{4+}$ and $19LE^{5+}$, the ejection of multiple, consecutive proton-bound dimers is measured. Exceptional stability of LE proton-bound dimers has previously been observed by Schnier et al. who measured the activation energy for dissociation of LE proton-bound dimers to be 1.6 ± 0.1 eV [39].

The ejection of proton-bound dimers and protonated monomers, and the absence of protonated trimers, seems to indicate that, unlike certain helical peptides [47, 54], a maximum of two LE monomers are able to solvate a proton. A possible test to confirm this would be to measure the activation energy of neutral loss from protonated LE trimers and tetramers and compare the values with the activation energy of a proton bound dimer. If the activation energy of protonated trimers and tetramers is substantially less than 1.6 eV, the third LE peptide in the cluster is probably not interacting directly with the proton. This value would also provide an estimate of the activation energy for evaporation of a LE monomer from a cluster.

It was shown previously that conformational flexibility plays a major role in the dissociation of protein homodimers [36]. The dissociation pathways of oxidized and reduced $5ST^{4+}$ are identical although the branching ratios between fission and evaporation are different, with the reduced $5ST^{4+}$ having a higher probability of neutral ST evaporation. This indicates the conformational flexibility of subunits in the cluster plays a role in ST cluster dissociation.

Cluster Dissociation and the Liquid-Drop Model

Probably the most widely used model to explain the dissociation of multiply charged clusters is the liquid-drop model originally formulated by Lord Rayleigh [55] and later refined and extended for nuclear fission [42]. In the liquid-drop model, a cluster is treated as an incompressible fluid in which individual monomer units are bound together by surface tension arising from short-range, and even nearest-neighbor, attractive interactions. Long-range coulombic repulsion between like charges within the cluster cause surface distortions that can lead to spontaneous fission, provided the cluster has sufficient charge or temperature [55]. In the liquid-drop model, large clusters of low charge have a high barrier to spontaneous fission and tend to dissociate by the evaporation of neutral components. As a cluster with constant charge decreases in size, the barrier towards spontaneous fission tends to decrease, eventually becoming competitive with the evaporation energy, and the cluster undergoes charge separation by fission [6].

The liquid-drop model has been adapted by various researchers to explain the dissociation processes of multiply charged systems as diverse as atomic nuclei [42], van der Waals clusters [56], and alkali [37, 57, 58] and noble metal clusters [5, 6]. The analogy between these clusters and liquid drops is justified by the cluster's approximately constant densities and fixed boundaries [6]. Clusters of the amino acids arginine [18] and serine [20, 27] have also been measured to undergo dissociation by neutral evaporation and charge separation by fission, although the liquid-drop model was not applied to these clusters.

The dissociation processes of multiply charged noble metal clusters [5–8, 59] is empirically similar to the dissociation of LE. In noble metal cluster dissociation, evaporation of a neutral metal atom competes with asymmetric fission, which is typically the ejection of a positively charged trimer or other small species. The observed fission products are known to have enhanced stability due to electronic shell effects [60, 61]. In metal cluster dissociation, the dominant dissociation process is determined by the charge of the cluster and the number of monomer units composing the cluster. Saunders showed that the log of the fission and evaporation ratio varies linearly with z^2/n, where z is the charge of the cluster and n is the number of monomer units in the cluster [5, 6]. This relation is also found for nuclear decay [43], leading Saunders to suggest that similar physical principles govern the behavior of multiply charged metal clusters and atomic nuclei [6].

The results of LE cluster dissociation presented in this study qualitatively resemble the dissociation of metal clusters and atomic nuclei. Instead of the evaporation of a neutral metal ion or a neutron, LE clusters evaporate a neutral peptide, and instead of undergoing charge separation by nuclear fission or the ejection of a metal trimer, LE clusters eject a proton-bound dimer or protonated monomer. The variation of the branching ratios of the various dissociation pathways of LE clusters with z^2/n is presented in Figure 9a. The primary dissociation pathway of LE clusters is neutral evaporation at low values of z^2/n. For example, $9LE^{2+}$, which has a z^2/n value of 0.44, dissociates by ~87% evaporation and ~13% fission. In contrast, $8LE^{2+}$, which has a z^2/n value of 0.5 dissociates by ~6% evaporation and ~94% fission. At the highest values of z^2/n in Figure 9a, corresponding to $15LE^{4+}$ and $19LE^{5+}$ with z^2/n values of 1.07 and 1.32, respectively, an additional fission pathway consisting of the ejection of protonated LE monomer occurs with a branching ratio as high as 16% for $19LE^{5+}$.

The most striking feature of Figure 9a is the sharp transition that occurs between dissociation primarily by evaporation of neutral LE to dissociation primarily by the ejection of a proton-bound dimer at a z^2/n value ~0.47. Similar sharp transitions between dissociation primarily by evaporation to dissociation primarily by fission have been measured for clusters of other materials. For doubly charged sodium clusters with thirty atoms, the transition occurs at a z^2/n ~0.13 [37], doubly charged gold clusters with fourteen atoms at a z^2/n ~0.29 [5, 6], doubly protonated arginine clusters with 12 amino acids [25] which corresponds to a z^2/n value of ~0.33, and uranium nuclei with 234 nucleons at a

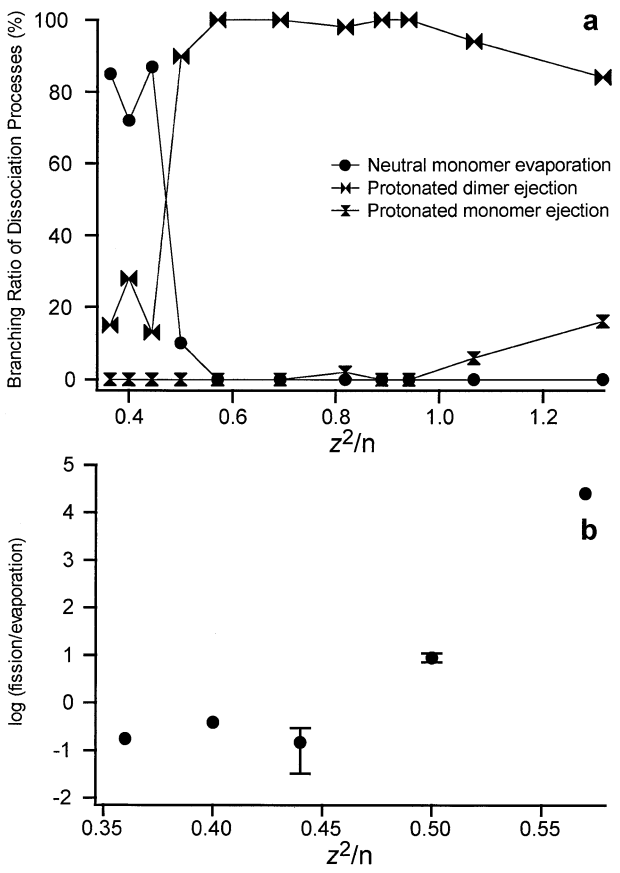

Figure 9. The dissociation pathways of LE clusters as a function of z^2/n where z is the charge and n is the cluster number for (**a**) the percentage of evaporation, fission by the ejection of $2LE^+$ and fission by the ejection of LE^+ produced by all clusters studied and (**b**) the log of the fission to evaporation ratio for the doubly protonated clusters studied. Error bars representing $\pm$ 1 σ are included in (**b**) for two data points.

z^2/n of 36.2 [43]. For doubly charged metal clusters the z^2/n value corresponding to the crossover value between dissociation primarily by evaporation and primarily by fission, is expected to correlate with the surface tension of the metal, where higher z^2/n values correspond to higher surface tensions [6]. Correlating trends in the crossover between dissociation by evaporation and fission to other materials, such as peptides or amino acids, is problematic due to the significant difference in both the size and charge density of the clusters. An interesting test of the application of the liquid drop model to amino acid and peptide clusters would be to measure the z^2/n values for the crossover in dissociation from primarily evaporation to fission for a series of clusters with the same charge and similar cross sections. A correlation between the z^2/n value of the crossover between evaporation and fission to the activation energy of dissociation would provide supporting evidence for the utility of applying the liquid-drop model to amino acid and peptide clusters.

Although the application of the liquid-drop model to qualitatively describe the dissociation processes of LE clusters is intriguing, some significant deviations from the model occur. According to the liquid-drop model of cluster dissociation, the barrier for cluster fission decreases rapidly, while the evaporation energy for neutral loss remains relatively constant with changing z^2/n. For a series of doubly charged LE clusters with different numbers of monomers and z^2/n values ranging from 0.36 to 0.57, the fission barrier decreases as the value of z^2/n increases. At z^2/n values were the fission barrier is comparable to the evaporation energy, fission is competitive with evaporation. This is well illustrated for doubly charged gold clusters [5, 6] and isotopes of uranium nuclei [43] by linear increases in plots of the log(fission/evaporation) with increasing z^2/n for these clusters. A similar plot for doubly charged LE clusters is presented in Figure 9b. For z^2/n values of 0.44 to 0.57, the increase in log(fission/evaporation) is very rapid, while at lower z^2/n values, the fission/evaporation ratio tends to level off to a value of 10–20% evaporation by fission. A similar leveling off of the fission/evaporation ratio to a value of 10–20% fission was measured for doubly charged clusters of antimony [38]. Brechignac et al. explained this result by suggesting that instead of continuing to increase with increasing cluster size, the fission barrier height evolves in such a way as to stay competitive with evaporation as the cluster size increases [38]. The interpretation of the LE cluster dissociation results would be greatly facilitated by the measurement of the activation energies of evaporation and fission for these clusters as has been reported for multiply charged silver clusters [62].

The liquid-drop model has been used previously to describe the asymmetric dissociation and charge partitioning of tetrameric streptavidin [30]. Homogeneous protein complexes of 2–6 monomer units have been shown to dissociate primarily by the ejection of a single subunit that removes 30–50% of the total charge of the complex [29–33, 35]. Schwartz et al. suggested that treating the protein complex as a liquid drop would explain some of the preferential charging for the ejected subunit as the surface-area-to-mass of the ejected subunit would be greater than that of the remaining cluster [30]. In the same paper, Schwartz et al. noted that the liquid-drop model could not account quantitatively for the magnitude of the charge enrichment of the leaving subunit. Subsequent work with protein homodimers has shown that other factors, such as protein conformational flexibility, the charge state of the protein complex, and the initial conformation of the protein complex play a dominant role in the dissociation pathways of protein homodimers [36]. These properties are not represented in the standard liquid-drop model and lead to significant differences between the dissociation of protein complexes and gold clusters.

Some of these same factors, such as conformational flexibility and multiple charging, of peptides within the cluster may be expected to cause deviations in cluster dissociation from the predictions of the liquid-drop model. Deviations from the liquid-drop model due to

conformational flexibility are indicated by differences in the branching ratios for evaporation and fission in the dissociation of oxidized and reduced $5ST^{4+}$ (Figure 8a, b). It is interesting that the application of a model as simple as the liquid-drop model to clusters of molecules as complex as amino acids and peptides yields any useful predictions or trends. As it is, results of the DR experiments of these peptide clusters suggest that the dissociation pathways of LE clusters, and to a lesser extent ST clusters, can be described reasonably well by a simple model where dissociation is determined primarily by the collective properties of cluster size and charge.

The Use of Double Resonance in Dissociation Experiments

Without the use of DR, the interpretation of dissociation spectra can be quite challenging. The dissociation spectrum of $9LE^{2+}$ (Figure 4a) has a large number of dissociation products with very different peak intensities for complimentary fragment ions. DR revealed that there are actually only two significant dissociation pathways and that the additional fragment ion peaks and seemingly uncorrelated peak intensities arise from subsequent dissociation. Determining dissociation pathways without the use of DR is challenging, but has been done nicely in some instances. For example, Cooks and coworkers studied the dissociation of serine octamers as a function of collision energy and observed that at gentle dissociation energies, protonated serine hexamer is the first fragment ion to appear with protonated pentamers and tetramers appearing at successively higher collision energies [27]. These results strongly suggest that protonated serine pentamers and hexamers are formed by sequential evaporation of neutral serine. In many other instances, it is extremely difficult to distinguish between primary and secondary fragment ions in dissociation spectra. These results clearly show the advantages of using DR wherever feasible in the study of cluster dissociation.

Conclusions

Cluster dissociation has been studied for a variety of atomic and molecular species, such as atomic nuclei, solvent microdroplets, metal clusters and amino acids, with an aim to both understand fundamental cluster properties and to "bridge-the-gap" between bulk and molecular properties. In this study, we extend the field of cluster dissociation to peptides by elucidating the dissociation pathways of leucine enkephalin (LE) clusters with 2–5 charges and multiply protonated somatostatin (ST) clusters formed with the peptide disulfide bonds either broken or intact. The peptide clusters were dissociated by collisional activation and the dissociation pathways were elucidated by double resonance experiments.

Clusters of both LE and ST dissociate by competing pathways of the evaporation of neutral peptides and coulombically driven fission. In the case of doubly protonated LE clusters, the significant parameter that determines the branching ratio of evaporation and fission is z^2/n, where z is the cluster charge and n is the number of monomer units in the cluster. Low values of z^2/n correlate to dissociation primarily by neutral evaporation while high values correlate to dissociation primarily by a fission process in which a LE proton-bound dimer is ejected. A sharp transition between dissociation primarily by evaporation and primarily by fission occurs at a z^2/n value of $\sim$0.47 for doubly protonated LE clusters. LE clusters with more than two protons dissociate by fission for the z^2/n values examined in these experiments. The dominant cluster fission process is the consecutive ejection of proton-bound dimers although significant amounts of protonated monomers are also observed in the fission processes of clusters with the highest z^2/n values studied. Fission results in the ejection of either protonated monomers or dimers indicating that no more than two LE peptides solvate a proton in these clusters. For ST pentamers with four protons, similar competing pathways for evaporation and fission by the ejection of protonated monomer are observed. Breaking the intermolecular disulfide bond of each peptide in the cluster changes the relative contributions of the two pathways, but no new pathways are observed.

The observation of two competing dissociation processes, with their relative abundances correlated to their z^2/n values, shows that the dissociation of LE clusters bears a qualitative similarity with nuclear and metal cluster dissociation. This similarity strongly suggests that the dissociation process of the LE clusters is determined by bulk properties of the cluster, namely the cluster charge state and size. Molecular properties do play at least some roll in the dissociation of peptide clusters as indicated by an increase in the branching ratio for ST cluster dissociation by evaporation when the molecular gas-phase conformational flexibility is increased.

The LE and ST clusters examined in this study are non-specific clusters, meaning that they do not have a physiologically relevant cluster structure in solution and show no evidence of magic number clustering in the gas phase. The branching ratios for the dissociation pathways of these clusters seem to be determined by the cluster size and charge as well as the product ion stability. These are the same factors that influence the dissociation of multiply charged clusters of gold atoms. It would be interesting to compare these results to those obtained for conformationally specific clusters where the specific conformations of these clusters may play a very significant role in determining their dissociation pathways.

Acknowledgments

A transmitter board and HI-222 chip were generously provided to the authors by Bruker Daltonics (Billerica, MA). The authors would like to thank Dr. Michael Leavell (Sandia National Laboratory, Livermore, CA), Dr. Julie Leary (University of California, Berkeley), and Mr. Scott Daniels and Dr. Christian Berg (Bruker Daltonics, Billerica, MA) for their assistance in modifying the mass spectrometer for double resonance experiments. Funding for this work was provided by the National Institutes of Heath (grant R01-GM64712-01).

References

1. Stace, A. J. Metal Ion Solvation in the Gas Phase: The Quest for Higher Oxidation States. *J. Phys. Chem. A* **2002,** *106,* 7993–8005.
2. Taflin, D. C.; Ward, T. L.; Davis, E. J. Electrified Droplet Fission and the Rayleigh Limit. *Langmuir* **1989,** *5,* 376–384.
3. Grimm, R. L.; Beauchamp, J. L. Evaporation and Discharge Dynamics of Highly Charged Droplets of Heptane, Octane, and p-Xylene Generated by Electrospray Ionization. *Anal. Chem.* **2002,** *74,* 6291–6297.
4. Sattler, K.; Muhlbach, J.; Echt, O.; Pfau, P.; Recknagel, E. Evidence for Coulomb Explosion of Doubly Charged Microclusters. *Phys. Rev. Lett.* **1981,** *47,* 160–163.
5. Saunders, W. A. Fission and Liquid-Drop Behavior of Charged Gold Clusters. *Phys. Rev. Lett.* **1990,** *64,* 3046–3049.
6. Saunders, W. A. Metal-Cluster Fission and the Liquid-Drop Model. *Phys. Rev. A* **1992,** *46,* 7028–7041.
7. Ziegler, J.; Dietrich, G.; Kruckeberg, S.; Lutzenkirchen, K.; Schweikhard, L.; Walther, C. Multicollision-Induced Dissociation of Multiply Charged Gold Clusters, Au-$n(2+)$, n = 7–35, and Au-$n(3+)$, n = 19–35. *Int. J. Mass Spectrom.* **2000,** *202,* 47–54.
8. Kruckeberg, S.; Schweikhard, L.; Dietrich, G.; Lutzenkirchen, K.; Walther, C.; Ziegler, J. Decay Pathway Determination of Even-Size Dicationic Silver Clusters: Ag-16(2+) and Ag-18(2+) Revisited by Pre-Precursor Selection and Sequential Decay. *Chem. Phys.* **2000,** *262,* 105–113.
9. Blades, A. T.; Jayaweera, P.; Ikonomou, M. G.; Kebarle, P. Ion-Molecule Clusters Involving Doubly Charged Metal-Ions (M2+). *Int. J. Mass Spectrom. Ion Processes* **1990,** *102,* 251–267.
10. Rodriguez-Cruz, S. E.; Jockusch, R. A.; Williams, E. R. Hydration Energies of Divalent Metal Ions, Ca2 + (H2O)(n) (n = 5–7) and Ni2 + (H2O)(n) (n = 6–8), obtained by blackbody infrared radiative dissociation. *J. Am. Chem. Soc.* **1998,** *120,* 5842–5843.
11. Walker, N. R.; Wright, R. R.; Barran, P. E.; Cox, H.; Stace, A. J. Unexpected stability of Cu·Ar (2+), Ag·Ar (2+), Au·Ar (2+), and their larger clusters. *J. Chem. Phys.* **2001,** *114,* 5562–5567.
12. Ditmire, T.; Tisch, J. W. G.; Springate, E.; Mason, M. B.; Hay, N.; Marangos, J. P.; Hutchinson, M. H. R. High Energy Ion Explosion of Atomic Clusters: Transition from Molecular to Plasma Behavior. *Phys. Rev. Lett.* **1997,** *78,* 2732–2735.
13. Kumarappan, V.; Krishnamurthy, M.; Mathur, D. Asymmetric High-Energy Ion Emission from Argon Clusters in Intense Laser Fields. *Phys. Rev. Lett.* **2001,** *87,* article no. 085005.
14. Snyder, E. M.; Wei, S.; Purnell, J.; Buzza, S. A.; Castleman, A. W. Femtosecond Laser-Induced Coulomb Explosion of Ammonia Clusters. *Chem. Phys. Lett.* **1996,** *248,* 1–7.
15. Card, D. A.; Wisniewski, E. S.; Folmer, D. E.; Castleman, A. W. Dynamics of Coulomb Explosion and Kinetic Energy Release in Clusters of Heterocyclic Compounds. *J. Chem. Phys.* **2002,** *116,* 3554–3567.
16. Pruvost, L.; Serre, I.; Duong, H. T.; Jortner, J. Expansion and Cooling of a Bright Rubidium Three-Dimensional Optical Molasses. *Phys. Rev. A* **2000,** *6105,* 053408.
17. Zhan, D. L.; Rosell, J.; Fenn, J. B. Solvation Studies of Electrospray Ions—Method and Early Results. *J. Am. Soc. Mass Spectrom.* **1998,** *9,* 1241–1247.
18. Zhang, D. X.; Wu, L. M.; Koch, K. J.; Cooks, R. G. Arginine Clusters Generated by Electrospray Ionization and Identified by Tandem Mass Spectrometry. *Eur. Mass Spectrom.* **1999,** *5,* 353–361.
19. Lee, S. W.; Beauchamp, J. L. Fourier Transform Ion Cyclotron Resonance Study of Multiply Charged Aggregates of Small Singly Charged Peptides Formed by Electrospray Ionization. *J. Am. Soc. Mass Spectrom.* **1999,** *10,* 347–351.
20. Julian, R. R.; Hodyss, R.; Kinnear, B.; Jarrold, M. F.; Beauchamp, J. L. Nanocrystalline Aggregation of Serine Detected by Electrospray Ionization Mass Spectrometry: Origin of the Stable Homochiral Gas-Phase Serine Octamer. *J. Phys. Chem. B* **2002,** *106,* 1219–1228.
21. Counterman, A. E.; Valentine, S. J.; Srebalus, C. A.; Henderson, S. C.; Hoaglund, C. S.; Clemmer, D. E. High-Order Structure and Dissociation of Gaseous Peptide Aggregates that are Hidden in Mass Spectra. *J. Am. Soc. Mass Spectrom.* **1998,** *9,* 743–759.
22. Counterman, A. E.; Clemmer, D. E. Magic Number Clusters of Serine in the Gas Phase. *J. Phys. Chem. B* **2001,** *105,* 8092–8096.
23. Counterman, A. E.; Hilderbrand, A. E.; Barnes, C. A. S.; Clemmer, D. E. Formation of Peptide Aggregates During ESI: Size, Charge, Composition, and Contributions to Noise. *J. Am. Soc. Mass Spectrom.* **2001,** *12,* 1020–1035.
24. Guevremont, R.; Purves, R. W. High Field Asymmetric Waveform Ion Mobility Spectrometry-Mass Spectrometry: An Investigation of Leucine Enkephalin Ions Produced by Electrospray Ionization. *J. Am. Soc. Mass Spectrom.* **1999,** *10,* 492–501.
25. Zhang, D. X.; Koch, K. J.; Tao, A.; Cooks, R. G. Clustering of Amino Acids in the Gas Phase by Electrospray Ionization Mass Spectrometry. *Proceedings of the 48th ASMS Conference on MS and Allied Topics*; Long Beach, CA, June, 2000.
26. Koch, K. J.; Gozzo, F. C.; Zhang, D. X.; Eberlin, M. N.; Cooks, R. G. Serine Octamer Metaclusters: Formation, Structure Elucidation, and Implications for Homochiral Polymerization. *Chem. Commun.* **2001**, 1854–1855.
27. Cooks, R. G.; Zhang, D. X.; Koch, K. J.; Gozzo, F. C.; Eberlin, M. N. Chiroselective Self-Directed Octamerization of Serine: Implications for Homochirogenesis. *Anal. Chem.* **2001,** *73,* 3646–3655.
28. Koch, K. J.; Gozzo, F. C.; Nanita, S. C.; Takats, Z.; Eberlin, M. N.; Cooks, R. G. Chiral Transmission Between Amino Acids: Chirally Selective Amino Acid Substitution in the Serine Octamer as a Possible Step in Homochirogenesis. *Angew. Chem. Int. Ed.* **2002,** *41,* 1721–1724.
29. Light-Wahl, K. J.; Schwartz, B. L.; Smith, R. D. Observation of the Noncovalent Quaternary Associations of Proteins By Electrospray Ionization Mass Spectrometry. *J. Am. Chem. Soc.* **1994,** *116,* 5271–5278.
30. Schwartz, B. L.; Bruce, J. E.; Anderson, G. A.; Hofstadler, S. A.; Rockwood, A. L.; Smith, R. D.; Chilkoti, A.; Stayton, P. S. Dissociation of Tetrameric Ions of Noncovalent Streptavidin Complexes Formed by Electrospray Ionization. *J. Am. Soc. Mass Spectrom.* **1995,** *6,* 459–465.
31. Fitzgerald, M. C.; Chernushevich, I.; Standing, K. G.; Whitman, C. P.; Kent, S. B. H. Probing the Oligomeric Structure of an Enzyme by Electrospray Ionization Time-of-Flight Mass Spectrometry. *Proc. Natl. Acad. Sci. U.S.A.* **1996,** *93,* 6851–6856.
32. Zhang, Z. G.; Krutchinsky, A.; Endicott, S.; Realini, C.; Rechsteiner, M.; Standing, K. G. Proteasome Activator 11S REG or PA28: Recombinant REG αREG β Hetero-Oligomers are Heptamers. *Biochemistry U.S.A.* **1999,** *38,* 5651–5658.
33. Felitsyn, N.; Kitova, E. N.; Klassen, J. S. Thermal Decomposition of a Gaseous Multiprotein Complex Studied by Black-

body Infrared Radiative Dissociation. Investigating the Origin of the Asymmetric Dissociation Behavior. *Anal. Chem.* **2001,** *73,* 4647–4661.
34. Kitova, E. N.; Bundle, D. R.; Klassen, J. S. Thermal Dissociation of Protein–Oligosaccharide Complexes in the Gas Phase: Mapping the Intrinsic Intermolecular Interactions. *J. Am. Chem. Soc.* **2002,** *124,* 5902–5913.
35. Hanson, C. L.; Fucini, P.; Ilag, L. L.; Nierhaus, K. H.; Robinson, C. V. Dissociation of Intact Escherichia coli Ribosomes in a Mass Spectrometer—Evidence for Conformational Change in a Ribosome Elongation Factor g Complex. *J. Biol. Chem.* **2003,** *278,* 1259–1267.
36. Jurchen, J. C.; Williams, E. R. Origin of Asymmetric Charge Partitioning in the Dissociation of Gas-Phase Protein Homodimers. *J. Am. Chem. Soc.* **2003,** *125,* 2817–2826.
37. Brechignac, C.; Cahuzac, P.; Carlier, F.; Defrutos, M. Asymmetric Fission of Nan++ Around the Critical Size of Stability. *Phys. Rev. Lett.* **1990,** *64,* 2893–2896.
38. Brechignac, C.; Cahuzac, P.; Carlier, F.; Defrutos, M.; Leygnier, J.; Roux, J. P. Coulombic Fission and Evaporation of Antimony Cluster Ions. *J. Chem. Phys.* **1995,** *102,* 763–769.
39. Schnier, P. D.; Price, W. D.; Strittmatter, E. F.; Williams, E. R. Dissociation Energetics and Mechanisms of Leucine Enkephalin (M + H)(+) and (2M + X)(+) Ions (X = H, Li, Na, K, and Rb) Measured by Blackbody Infrared Radiative Dissociation. *J. Am. Soc. Mass Spectrom.* **1997,** *8,* 771–780.
40. Kunimura, M.; Sakamoto, S.; Yamaguchi, K. Alkali Metal-Mediated Proline Aggregation in Solution Observed by Cold-spray Ionization Mass Spectrometry. *Org. Lett.* **2002,** *4,* 347–350.
41. Last, I.; Levy, Y.; Jortner, J. Beyond the Rayleigh Instability Limit for Multicharged Finite Systems: From Fission to Coulomb Explosion. *Proc. Natl. Acad. Sci. U.S.A.* **2002,** *99,* 9107–9112.
42. Bohr, N.; Wheeler, J. A. The Mechanism of Nuclear Fission. *Phys. Rev.* **1939,** *56,* 426–450.
43. Halpern, I. Nuclear Fission. *Annu. Rev. Nucl. Sci.* **1959,** *9,* 245–341.
44. Versluis, C.; van der Staaij, A.; Stokvis, E.; Heck, A. J. R.; de Craene, B. Metastable Ion Formation and Disparate Charge Separation in the Gas-Phase Dissection of Protein Assemblies Studied by Orthogonal Time-of-Flight Mass Spectrometry. *J. Am. Soc. Mass Spectrom.* **2001,** *12,* 329–336.
45. Rostom, A. A.; Sunde, M.; Richardson, S. J.; Schreiber, G.; Jarvis, S.; Bateman, R.; Dobson, C. M.; Robinson, C. V. Dissection of Multi-Protein Complexes Using Mass Spectrometry: Subunit Interactions in Transthyretin and Retinol-Binding Protein Complexes. *Proteins* **1998**, Suppl. 2, 3–11.
46. Kogan, A.; Ustyuzhanin, P.; Reuben, B. G.; Lifshitz, C. Hydtrogen/Deuterium Exchange of Monomers and Dimers of Leucine Enkephalin. *Int. J. Mass Spectrom.* **2002,** *213,* 1–4.
47. Kaleta, D. T.; Jarrold, M. F. Noncovalent Interactions Between Unsolvated Peptides. *J. Phys. Chem. A* **2002,** *106,* 9655–9664.
48. Schalley, C. A.; Weis, P. Unusually Stable Magic Number Clusters of Serine with a Surprising Preference for Homochirality. *Int. J. Mass Spectrom.* **2002,** *221,* 9–19.
49. Anders, L. R.; Beauchamp, J. L.; Dunbar, R. C.; Baldeschwieler, J. D. Ion-Cyclotron Double Resonance. *J. Chem. Phys.* **1966,** *45,* 1062–1063.
50. Comisarow, M. B.; Grassi, V.; Parisod, G. Fourier-Transform Ion-Cyclotron Double-Resonance. *Chem. Phys. Lett.* **1978,** *57,* 413–416.
51. Asam, M. R.; Glish, G. L. Tandem Mass Spectrometry of Alkali Cationized Polysaccharides in a Quadrupole Ion Trap. *J. Am. Soc. Mass Spectrom.* **1997,** *8,* 987–995.
52. Gauthier, J. W.; Trautman, T. R.; Jacobson, D. B. Sustained Off-Resonance Irradiation for Collision-Activated Dissociation Involving Fourier-Transform Mass-Spectrometry—Collision-Activated Dissociation Technique that Emulates Infrared Multiphoton Dissociation. *Anal. Chim. Acta* **1991,** *246,* 211–225.
53. Wang, J.; Cassady, C. J. Effects of Disulfide Linkages on Gas-Phase Reactions of Small Multiply Charged Peptide Ions. *Int. J. Mass Spectrom.* **1999,** *182/183,* 233–241.
54. Kaleta, D. T.; Jarrold, M. F. Peptide Pinwheels. *J. Am. Chem. Soc.* **2002,** *124,* 1154–1155.
55. Lord Rayleigh, L. On the Equilibrium of Liquid Conducting Masses Charged with Electricity. Phil. Mag. 1882, 14, 184–186.
56. Echt, O.; Kreisle, D.; Recknagel, E.; Saenz, J. J.; Casero, R.; Soler, J. M. Dissociation Channels of Multiply Charged Vanderwaals Clusters. *Phys. Rev. A* **1988,** *38,* 3236–3248.
57. Yannouleas, C.; Landman, U.; Brechignac, C.; Cahuzac, P.; Concina, B.; Leygnier, J. Thermal Quenching of Electronic Shells and Channel Competition in Cluster Fission. *Phys. Rev. Lett.* **2002,** *89,* article no. 173403.
58. Saunders, W. A. Asymmetric Fission of Nan++ around the Critical Size of Stability—Comment. *Phys. Rev. Lett.* **1991,** *66,* 840–840.
59. Naher, U.; Bjornholm, S.; Frauendorf, S.; Garcias, F.; Guet, C. Fission of Metal Clusters. *Phys. Rep. Rev. Sec. Phys. Lett.* **1997,** *285,* 245–320.
60. Knight, W. D.; Clemenger, K.; Deheer, W. A.; Saunders, W. A.; Chou, M. Y.; Cohen, M. L. Electronic Shell Structure and Abundances of Sodium Clusters. *Phys. Rev. Lett.* **1984,** *52,* 2141–2143.
61. Nakamura, M.; Ishii, Y.; Tamura, A.; Sugano, S. Shell Effects on Symmetrical Fragmentations of Alkali-Metal Clusters. *Phys. Rev. A* **1990,** *42,* 2267–2278.
62. Kruckeberg, S.; Dietrich, C.; Lutzenkirchen, K.; Schweikhard, L.; Walther, C.; Ziegler, J. Fission Barriers of Doubly Charged Silver Clusters. *Eur. Phys. J. D* **1999,** *9,* 145–148.